Contribution from the Department of Chemistry,
Northern Illinois University, DeKalb, Illinois 60115

Electronic Absorption and MCD Spectra for the $Au_8(PPh_3)_8^{2+}$ Ion

Huey-Rong C. Jaw and W. Roy Mason*

Received March 1, 1991

Electronic absorption and magnetic circular dichroism (MCD) spectra in the vis-UV range 1.66-3.60 μm^{-1} are reported for $[Au_8(PPh_3)_8](NO_3)_2$ in acetonitrile solution at room temperature. The MCD spectrum consists of both *A* and *B* terms and adds important detail to a consideration of the absorption spectrum. The spectra are interpreted in terms of a MO model in which skeletal bonding in the C_{3v} cluster complex is described by σ interaction among 6s atomic orbitals of the gold atoms. The lowest energy excited states are ascribed to intraskeletal transitions. Evidence is also presented for a Au 5d → 6s skeletal transition in the spectra for $Au_8(PPh_3)_8^{2+}$. Differences observed between the spectra for $Au_9(PPh_3)_8^{3+}$ and $Au_8(PPh_3)_8^{2+}$ are also discussed.

Introduction

Centered gold cluster complexes of the general formula $Au(AuPPh_3)_n^{m+}$ are known to be highly colored substances, and they exhibit several intense absorption bands in the visible and near-UV region.[1] These electronic spectral bands, which are characteristic of the individual cluster complex, have been largely uninterpreted until recently when the absorption and magnetic circular dichroism (MCD) spectra for the green $Au_9(PPh_3)_8^{3+}$ ion were investigated in our laboratory.[2] The solution structure of this ion was assumed to be a *bicapped* centered chair (D_{2h} skeletal symmetry), and the absorption and MCD spectra were interpreted in terms of skeletal electronic transitions between orbitals composed primarily of Au 6s atomic orbitals. As an offshoot of this work and part of a continuing effort to characterize the spectra of gold cluster complexes, the absorption and MCD spectra were obtained for the red $Au_8(PPh_3)_8^{2+}$ ion (structure **1**; ligand phenyl groups omitted

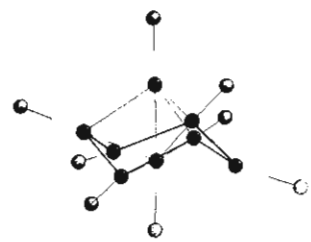

1

for clarity). The structure of this ion is related to that of $Au_9(PPh_3)_8^{3+}$ in that it can be viewed as a *monocapped* centered chair (C_{3v} skeletal symmetry) with one of the capping $AuPPh_3^+$ groups in $Au_9(PPh_3)_8^{3+}$ replaced by PPh_3 bound to the central Au.[3] It was not surprising at first glance that the general patterns of the absorption spectra for $Au_9(PPh_3)_8^{3+}$ and $Au_8(PPh_3)_8^{2+}$ were similar. However, the MCD spectra for the two ions are notably different. The present paper draws attention to the differences and offers some suggestions as to interpretation for the $Au_8(PPh_3)_8^{2+}$ spectra.

Experimental Section

The red octakis(triphenylphosphine)octagold nitrate, $[Au_8(PPh_3)_8](NO_3)_2$, was prepared according to the literature[3] by treating $[Au_9(PPh_3)_8](NO_3)_3$[4] with excess PPh_3 in either methanol or dichloromethane solution. The solid was recrystallized from 1:1 dichloromethane/ethyl ether. The compound gave satisfactory elemental analysis and a vis-UV spectrum that compared favorably with the published spectrum.[1]

Absorption spectra were measured for acetonitrile solutions by means of a Cary 1501 spectrophotometer. Absorption and MCD spectra were recorded simultaneously and synchronously along the same light path by means of a spectrometer described previously.[5] A magnetic field of 7.0 T was obtained from a superconducting magnet system (Oxford Instruments SM2-7, fitted with a room-temperature bore tube). Spectral grade acetonitrile was used throughout, and all spectra were corrected for solvent blank. Spectral measurements were limited to energies below 3.6 μm^{-1} because of strong absorptions from the phenyl substituents and the nitrate counterions. Absorption and MCD spectra obeyed Beer's law to within experimental error in the concentration range 10^{-4}-10^{-5} M. The solutions were not light sensitive and did not exhibit any changes during the time (typically 1 h) required to make the spectral measurements.

Table I. Spectral Data for $[Au_8(PPh_3)_8](NO_3)_2$ in CH_3CN

	absorption			MCD	
band no.	$\bar{\nu}$, μm^{-1}	λ, nm	ϵ, $(M\ cm)^{-1}$	$\bar{\nu}$, μm^{-1}	$\Delta\epsilon_M$, $(M\ cm\ T)^{-1}$
				1.98	+0.73
I	2.19	457	15 500	2.20	-1.13
II	2.43	412	18 500	2.38	+0.85
III	2.71	369	22 300[a]	2.51	+0.69[a]
				2.62	0
				2.76	-2.43
IV	3.00	333	45 000[a]	3.00	-3.86
V	3.23	310	68 000[a]	3.18	-4.32[b]
				3.26	-2.87[c]
VI	3.42	292	79 000	3.34	-3.96[b]
				3.49	-1.84[c]

[a] Shoulder. [b] Minimum. [c] Maximum.

Results and Discussion

Electronic Absorption and MCD Spectra. The electronic absorption and MCD spectra for $[Au_8(PPh_3)_8](NO_3)_2$ in acetonitrile solution at room temperature are presented on the left in Figure 1, together with a comparison to the spectra obtained previously for $[Au_9(PPh_3)_8](NO_3)_3$ in acetonitrile on the right. Quantitative spectral data for $Au_8(PPh_3)_8^{2+}$ are collected in Table I. As in the previous study of $Au_9(PPh_3)_8^{3+}$, the MCD spectrum for $Au_8(PPh_3)_8^{2+}$ adds important detail to the bands observed in the absorption spectrum. The bands labeled I-VI in Figure 1 all have high molar absorptivity ($\epsilon \sim 15\,500$-$79\,000\ M^{-1}\ cm^{-1}$) and are logically interpreted as allowed electronic transitions. Further, these bands are reasonably assigned to intramolecular transitions of the $Au_8(PPh_3)_8^{2+}$ cluster framework. They are unlikely to be due to absorptions by the ligand phenyl substitutents or the nitrate ions because the lowest energy bands observed for free PPh_3, coordinated PPh_3 (in $AuCl(PPh_3)$ for example), or NO_3^- are found above 3.6 μm^{-1}.

The solution structure of the $Au_8(PPh_3)_8^{2+}$ ion is not known, but the red color of the solid salts[3] is unchanged on dissolution in acetonitrile. Therefore, the solid-state structure of the $Au_8(PPh_3)_8^{2+}$ ion is assumed to be retained in solution and thus approximated by C_{3v} skeletal symmetry. With this assumption of C_{3v} symmetry in solution, electric dipole allowed transitions to degenerate E and nondegenerate A_1 excited states are anticipated. The former can exhibit MCD *A* terms resulting from Zeeman splitting of the degeneracy by the applied field.[6] Transitions to both E and A_1 states can exhibit *B* terms due to

(1) Hall, K. P.; Mingos, D. M. P. *Prog. Inorg. Chem.* **1984**, *32*, 237.
(2) Jaw, H.-R. C.; Mason, W. R. *Inorg. Chem.* **1991**, *30*, 275.
(3) (a) Manassero, M.; Naldini, L.; Sansoni, M. *J. Chem. Soc., Chem. Commun.* **1979**, 385. (b) Vollenbroek, F. A.; Bosman, W. P.; Bour, J. J.; Noordik, J. H.; Beurskens, P. T. *J. Chem. Soc., Chem. Commun.* **1979**, 387.
(4) Cariati, F.; Naldini, L. *J. Chem. Soc., Dalton Trans.* **1972**, 2286.
(5) Mason, W. R. *Anal. Chem.* **1982**, *54*, 646.
(6) For a review of MCD spectroscopy together with the standard (Stephens) definitions and conventions used here see: Piepho, S. B.; Schatz, P. N. *Group Theory in Spectroscopy with Applications to Magnetic Circular Dichroism*; Wiley-Interscience: New York, 1983.

0020-1669/91/1330-3552$02.50/0

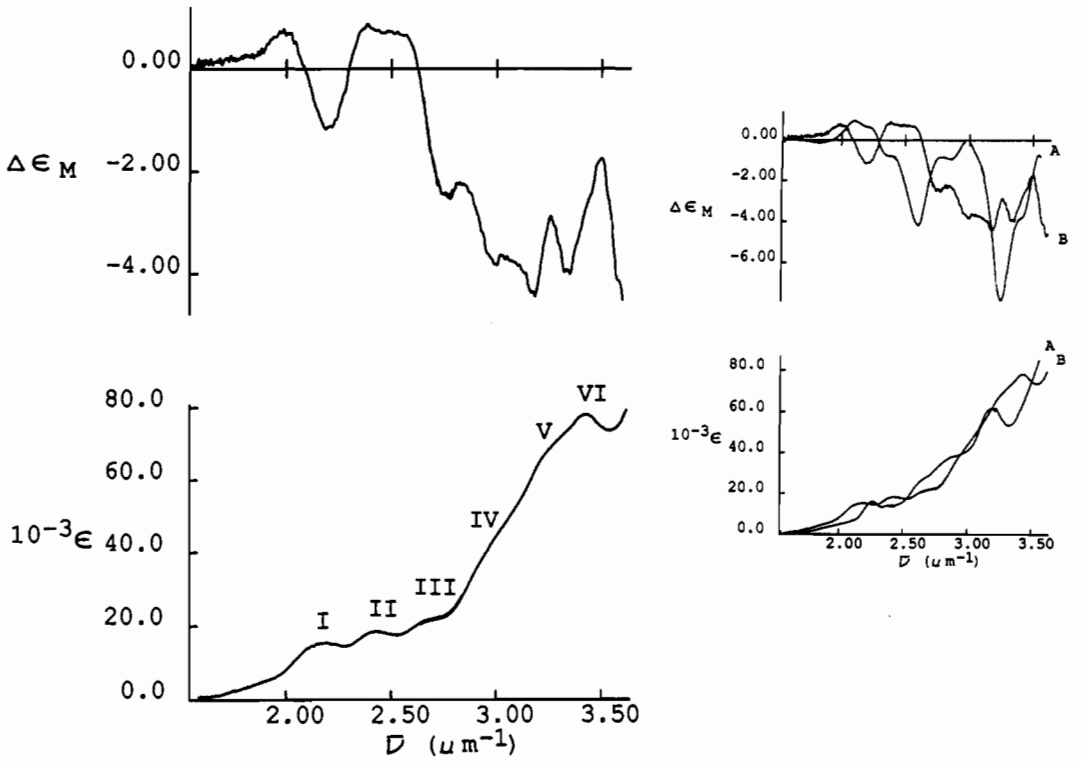

Figure 1. Electronic absorption (lower curves) and MCD (upper curves) spectra for $[Au_8(PPh_3)_8](NO_3)_2$ in acetonitrile (left) and a comparison of the absorption and MCD spectra for (A) $Au_9(PPh_3)_8^{3+}$ [2] and (B) $Au_8(PPh_3)_8^{2+}$ (this work) (right). $\Delta\epsilon_M$ has units of $(M\ cm\ T)^{-1}$.

field-induced mixing, but *C* terms will be absent because the molecular ground state is diamagnetic.[6] The negative and positive MCD features associated with bands I and II are likely due to *B* terms because the extrema are near the energy of the band maxima. The MCD maximum at 1.98 μm^{-1} demonstrates the presence of one or more transitions lower in energy than band I which are not resolved in the absorption spectrum. In the region 2.5–2.8 μm^{-1} the MCD has the appearance of a negative *A* term because $\Delta\epsilon_M = 0$ occurs near the energy of band III. In the 3.0–3.5-μm^{-1} region both the MCD and absorption for bands IV–VI appear to be influenced by strong broad features to higher energy. These strong features undoubtedly include, among other possibilities, absorptions by phenyl and NO_3^-, and it is possible that these absorptions tail into the 3.0–3.5-μm^{-1} region and are responsible for the lower resolution of bands IV–VI. This lower resolution and underlying background absorption complicate the interpretation of the spectra in this region. For example, the broad negative MCD shows oscillations consisting of minima and maxima that are to either side of the energies of bands V and VI. This behavior suggests positive *A* terms are present for these two bands. However, a term assignment for the poorly resolved band IV cannot be made with any confidence; the MCD feature occurs at essentially the same energy as the shoulder absorption.

The comparison of the $Au_8(PPh_3)_8^{2+}$ spectra with those obtained earlier[2] for $Au_9(PPh_3)_8^{3+}$ on the right side of Figure 1 shows clear differences in the MCD in signs, bandwidths, and resolution of individual features. The MCD for $Au_9(PPh_3)_8^{3+}$ is better resolved with narrower features than that for $Au_8(PPh_3)_8^{2+}$, especially in the 3.0–3.5-μm^{-1} region. On close inspection, similar differences are also observed in the absorption spectra of the two ions, but the differenes are less dramatic.

Energy Levels, Electronic States, and MCD Terms. The skeletal bonding in several gold cluster complexes has been described in terms of a simple Hückel MO model based on σ interaction among the Au 6s valence orbitals.[1,7] In this model, the filled 5d orbitals on the Au atoms are considered to be "corelike" and the empty Au 6p orbitals are assumed to be too high in energy to contribute significantly. The simple model was elaborated upon more recently[8] by means of extended Hückel MO calculations, but the essential features of the model were retained. Our earlier study of $Au_9(PPh_3)_8^{3+}$ showed that the model could provide a useful basis for spectral interpretation.[2] Therefore, an analogous MO scheme was constructed for the C_{3v} $Au_8(PPh_3)_8^{2+}$ ion investigated here. Figure 2 presents an energy level diagram suited to interpreting the spectra, and Table II lists the one-electron MO's used to construct the diagram. This level scheme is essentially the same as given in the earlier calculation,[8] but it differs from a scheme developed for a noncentered D_{2h} $Au_8L_8^{2+}$ complex.[7] The

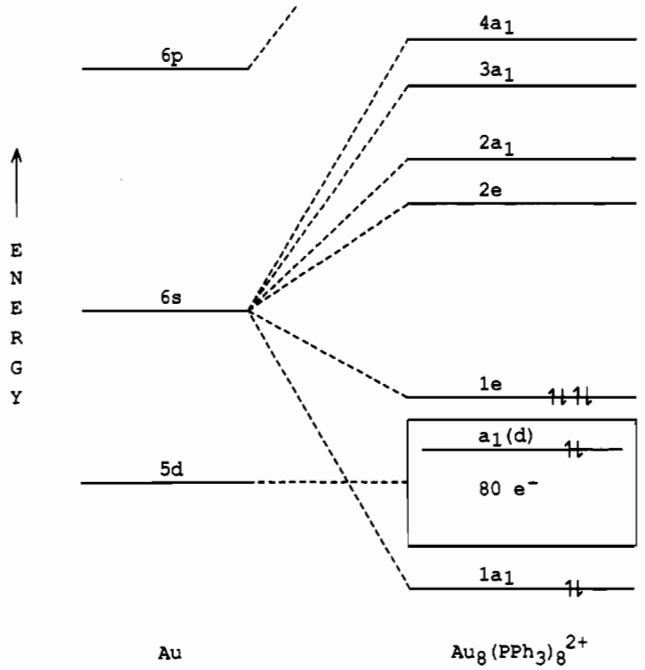

Figure 2. Molecular orbital energy levels for $Au_8(PPh_3)_8^{2+}$ based on the assumption of C_{3v} symmetry and primarily Au 6s skeletal bonding.

(7) Mingos, D. M. P. *J. Chem. Soc., Dalton Trans.* **1976**, 1163.

(8) Van der Velden, J. W. A.; Stadnik, Z. M. *Inorg. Chem.* **1984**, *23*, 2640.

Table II. One-Electron Molecular Orbitals

symm	energy[a]	MO wave function[b]
$1a_1$	$2.23\beta_1 + 1.87\beta_2$	$(1/2\sqrt{3})(\sqrt{3}\phi_1 + \sqrt{3}\phi_2 + \phi_3 + \phi_4 + \phi_5 + \phi_6 + \phi_7 + \phi_8)$
1e	$0.5\beta_2$	$(1/\sqrt{12})(2\phi_3 - \phi_4 - \phi_5 + 2\phi_6 - \phi_7 - \phi_8)$
		$(1/2)(\phi_4 - \phi_5 + \phi_7 - \phi_8)$
2e	$-0.5\beta_2$	$(1/\sqrt{12})(2\phi_3 - \phi_4 - \phi_5 - 2\phi_6 + \phi_7 + \phi_8)$
		$(1/2)(\phi_4 - \phi_5 - \phi_7 + \phi_8)$
$2a_1$	$-0.5\beta_1 - 0.13\beta_2$	$(1/2\sqrt{3})(\sqrt{3}\phi_1 - \sqrt{3}\phi_2 - \phi_3 - \phi_4 - \phi_5 + \phi_6 + \phi_7 + \phi_8)$
$3a_1$	$-1.23\beta_1 + 0.13\beta_2$	$(1/2\sqrt{3})(\sqrt{3}\phi_1 + \sqrt{3}\phi_2 - \phi_3 - \phi_4 - \phi_5 - \phi_6 - \phi_7 - \phi_8)$
$4a_1$	$-0.5\beta_1 - 1.87\beta_2$	$(1/2\sqrt{3})(\sqrt{3}\phi_1 - \sqrt{3}\phi_2 + \phi_3 + \phi_4 + \phi_5 - \phi_6 - \phi_7 - \phi_8)$

[a] Hückel MO exchange integrals: β_1 from radial overlap of ϕ_1 with ϕ_2, ϕ_3, ..., ϕ_8; β_2 from adjacent tangential overlap ϕ_2, ϕ_3; ϕ_3, ϕ_4; etc. [b] ϕ_i = Au 6s orbital on atom i.

Table III. Excited Configurations and States

excited confgn[a]	zero-order states	spin–orbit states[b]	$\bar{A}_1/\bar{D}_0$[c]
$(1e)^3(2e)$	$^1A_1$	$1A_1$	
	$^3A_1$	$(1A_2)$, 1E	pos
	$^1A_2$	$(2A_2)$	
	$^3A_2$	$2A_1$, 2E	pos
	^1E	3E	~0
	^3E	4E, $3A_1$	~0
		$(3A_2)$, 5E	neg
$(1e)^3(2a_1)$	^1E	6E	pos
	^3E	7E, $4A_1$	pos
		$(4A_2)$, 8E	~0

[a] Filled orbitals omitted. Ground-state configuration: ... $(1e)^4$, $^1A_1$. [b] Electric dipole forbidden A_2 states in parentheses. [c] Estimated from eq 1 for E states.

ground-state configuration for $Au_8(PPh_3)_8^{2+}$ is assumed to be $(1a_1)^2(Au\ 5d)^{80}(1e)^4$ and therefore is diamagnetic and designated $^1A_1$. The lowest energy excited configurations are reasonably ascribed to excitations from 1e (HOMO) to 2e (LUMO) or $2a_1$. Table III lists the excited states associated with these configurations. Because of strong Au spin–orbit coupling, the zero-order singlet and triplet states will become intermixed and the resulting spin–orbit states, characterized by the lack of spin-multiplicity superscripts, will provide the basis for spectral interpretation.

MCD A terms for the degenerate E(i) excited states can be given in terms of the $\bar{A}_1/\bar{D}_0$ parameter ratio for space-averaged nonisotropic molecules in solution by eq 1,[6] where $\bar{D}_0 = (1/3)|\langle A_1||\mathbf{m}||E(i)\rangle|^2$ is related to the electric dipole strength of the transition to the E(i) state, μ_B is the Bohr magneton, $\mu = -\mu_B(\mathbf{L} + 2\mathbf{S})$, and $\mathbf{m} = e\mathbf{r}$, the magnetic and electric moment operators in the respective reduced matrix elements (RME's). The E(i) states (Table III) are defined in terms of antisymmetrized one-electron MO's and are thus approximated by Au atomic orbitals. In the present analysis, the ϕ_i were assumed to be Au 6s orbitals (Table II), although an in-pointing 6s6p σ-hybrid could just as well be used without affecting the basic arguments. The orbital (**L**) part of the magnetic moment RME in eq 1 is therefore due entirely to two-centered contributions because a 6s orbital on a single Au center has no angular momentum and therefore no magnetic moment. The two-centered orbital angular momentum terms necessary to evaluate the RME in eq 1 were approximated by the relation[2,9]

$$\langle \phi_i | l_z | \phi_j \rangle = -iT_{ij}(x_i y_j - y_i x_j)$$

where T_{ij} is an overlap integral between ϕ_i and ϕ_j (assumed to be positive for positive phases for ϕ_i and ϕ_j) and x, y, and z are Cartesian coordinates of atom i and j referred to the center of the coordinate system. The use of eq 1 here is to attempt to predict the *sign* of the A terms anticipated for the E(i) states; a quantitative calculation of the $\bar{A}_1/\bar{D}_0$ magnitude is probably not very reliable in view of the approximations involved. The signs expected for the E(i) states derived from eq 1 are given in Table III. The values listed there as ~0 result from the summation of equal terms of opposite sign and are at least expected to be very small. For example, the orbital angular momentum from 1e is equal and opposite in sign to that from 2e, which results in zero orbital angular momentum for the $(1e)^3(2e)$ 3E spin–orbit state of predominantly ^1E parentage.

The B term for an A_1 or an E(i) state of interest arises from a summation of magnetic interactions with all other E(j) states in the applied field and will be proportional to RME's of the type $\langle A_1||\mu||E(j)\rangle$ or $\langle E(i)||\mu||E(j)\rangle$ and inversely proportional to the energy differences between the interacting states and the state of interest.[6] Because of this summation, the prediction of B term signs is a difficult task unless the number of interacting states can be limited to only a few, for example those closest in energy to the state of interest. In the present case, the states closest to those of interest (those of Table III) were found to have very small RME's, and therefore many terms from higher energy configurations should be included in the summation. Consequently, after some preliminary calculations on the predominantly singlet states of Table III, it was concluded that the determination of B term signs in the present case is unfortunately not feasible. For the E states where the A terms are expected to be small (see above), the B term, whatever its sign, will likely determine the observed MCD.

Spectral Interpretation. On the basis of energy and intensity, bands I and II of the absorption spectrum for $Au_8(PPh_3)_8^{2+}$ are assigned to transitions to the spin–orbit states of the lowest energy $(1e)^3(2e)$ excited configuration of predominantly singlet origin, $1A_1(^1A_1)$ and $3E(^1E)$, respectively (Table III). The transition to the electric dipole forbidden $2A_2(^1A_2)$ state is expected to be at similar energy but is too weak to be observed. The absence of a prominent A term for the 3E state is rationalized by the very small $\bar{A}_1/\bar{D}_0$ predicted from eq 1; the MCD for bands I and II is interpreted as due to B terms. The spin–orbit states of predominantly triplet parentage [$1E(^3A_1)$; $2E$ and $2A_1(^3A_2)$; 4E, 3A, and $5E(^3E)$] are all expected 0.2–0.5 μm^{-1} lower in energy than band I or II, and transitions to them are expected to be weak.[2] The MCD maximum at 1.98 μm^{-1} and the red tail in the absorption spectrum below the energy of band I are ascribed to these states. Unfortunately, the lack of resolution of individual bands, which precludes MCD term assignments, dictates that little interpretive insight can be obtained from this region. The negative A term expected for 5E could be partly responsible for the 1.98-μm^{-1} maximum if it overlaps the observed negative B term for band I, but to suggest further detail from the present results would be even more speculative.

The higher energy absorption maximum at 3.42 μm^{-1}, band VI, is assigned as the transition to the $6E(^1E)$ state of the next higher energy excited configuration $(1e)^3(2a_1)$. As discussed above, the oscillation in the MCD spectrum that surrounds the band VI maximum is taken as evidence for the positive A term expected for the 6E state. The two ill-defined absorption shoulders at 3.0 μm^{-1}, band IV, and 3.23 μm^{-1}, band V, are then logically interpreted as due to transitions to states of ^3E parentage: $4A_1/8E$ and 7E, respectively. These assignments are reasonable in view of their lower energy compared to that of band VI and their lower intensity, which is reflected by their poor resolution. The oscillation in the MCD spectrum near the position of band V is ascribed to the positive A term expected for 7E, while the lack of such a clear oscillation near band IV suggests the absence of a significant A term, consistent with 8E.

The assignment of band III at 2.7 μm^{-1} remains to be discussed. If the observed MCD feature in the 2.5–2.8-μm^{-1} region is interpreted as a negative A term as it appears, then with the exception of 5E the E states of Table III cannot provide a suitable explanation for band III. Attempts were made to assign bands I, II, and IV–VI in such a way as to associate 5E with band III,

(9) VanCott, T. C.; Rose, J. L.; Misener, G. C.; Williamson, B. E.; Schrimpf, A. E.; Boyle, M. E.; Schatz, P. N. *J. Phys. Chem.* **1989**, *93*, 2999.

but such a scheme would require the zero-order singlet–triplet energy separations to be unrealistically large (>0.7 μm^{-1} in some cases) and transition intensities for states of triplet origin to be too high. An alternative possibility, and one favored here, is that band III and the associated negative *A* term are derived from an excitation from the essentially nonbonding Au 5d orbitals to 2e (see Figure 2). Simple reasoning places an a_1 symmetry combination of $5d_{z^2}$ orbitals at the top of the 5d band. This combination would be constructed in a manner analogous to $4a_1$ by assuming weak σ interactions among the $5d_{z^2}$ orbitals on the Au atoms of the cluster complex. A predominantly singlet excitation to 2e from this $a_1(d)$ orbital would give an E state with orbital magnetic moment due entirely to the 2e skeletal orbital leading to a negative *A* term. If this assignment for band III is accepted, then some of the broadening in the 3.0–3.5-μm^{-1} region could be rationalized as due to other unresolved and underlying 5d → 2e transitions. The presence of one or more 5d → 2e transitions for $Au_8(PPh_3)_8^{2+}$ also provides an explanation for the differences noted in the comparison with the $Au_9(PPh_3)_8^{3+}$ spectra, where no 5d → 6s skeletal transitions were assigned below ~3.5 μm^{-1}.[2] The presence of such transitions to lower energy in the $Au_8(PPh_3)_8^{2+}$ spectra can be explained by assuming a smaller 5d–6s atomic orbital energy difference for the Au atoms of the lower charged cluster complex. The lower charge on the complex will certainly reduce the extent of Ph_3P → Au donation, which in turn will stabilize the 6s skeletal orbitals relative to 5d. Furthermore, atomic spectral data[10] show that the Au 5d–6s orbital energy difference in the absence of ligand influence increases strongly with charge on Au and ranges from 1.4 μm^{-1} for Au^0 to 2.9 μm^{-1} for Au^+. Thus a "red shift" of 5d → 6s skeletal transitions compared to the 6s intraskeletal transitions seems plausible for $Au_8(PPh_3)_8^{2+}$ compared to $Au_9(PPh_3)_8^{3+}$. If this reasoning is correct, transitions involving the 5d orbitals may also appear in the spectra of other more "reduced" cluster complexes, such as the red $Au_9(PPh_3)_8^{+}$, for example.[1] MCD spectra seem to be a useful probe of such transitions that cannot be easily identified on the basis of the absorption spectra alone. Further investigation of the MCD spectra of "reduced" cluster complexes is presently underway in our laboratory.

Concluding Remarks. The MO scheme of Figure 2, which describes the skeletal bonding among the Au atoms in terms of primarily 6s σ interactions, has the capability of providing a basis for a logical interpretation of the absorption and MCD spectra for the $Au_8(PPh_3)_8^{2+}$ ion. This scheme is similar to that used earlier for the $Au_9(PPh_3)_8^{3+}$ ion.[2] It must be admitted however that the "density" of low-energy excited states that can be visualized for these cluster complexes is high, especially when the 5d → 6s skeletal excitations are included. Therefore, the present spectral assignments for $Au_8(PPh_3)_8^{2+}$ may not be unique. However, the assignments proposed have the advantage of simplicity and internal consistency. The differences between the spectra for $Au_8(PPh_3)_8^{2+}$ and those for $Au_9(PPh_3)_8^{3+}$ can be explained on the basis of (1) changes in the skeletal MO's due to different molecular symmetries (C_{3v} vs D_{2h}) and (2) the presence of the "red-shifted" 5d → 6s skeletal transition in the $Au_8(PPh_3)_8^{2+}$ spectra. The molecular symmetry differences in the MO schemes for the two ions are described primarily by the collapse of pairs of separated, nondegenerate D_{2h} orbitals to give the 1e and 2e degenerate C_{3v} orbitals. Such shifts of the one-electron MO's are likely responsible for the slight red shift of the lowest energy absorption bands of $Au_8(PPh_3)_8^{2+}$ compared to those of $Au_9(PPh_3)_8^{3+}$ and thus account for the color difference between the two complex ions. The 5d → 6s skeletal transition among the 6s intraskeletal transitions in $Au_8(PPh_3)_8^{2+}$ is interesting and emphasizes a spectroscopic role for the nonbonding Au 5d orbitals in the cluster complex. The skeletal bonding is still visualized as due predominantly to the 6s σ interactions. As pointed out earlier,[2] these σ interactions are enhanced by the relativistic stabilization and radial contraction of the Au 6s orbitals.[11]

Acknowledgment is made to the donors of the Petroleum Research Fund, administered by the American Chemical Society, for support of this work.

(10) Moore, C. E. *Natl. Bur. Stand. Circ. (U.S.)* **1958**, *No. 467*, Vol. III.

(11) Pyykkö, P. *Chem. Rev.* **1988**, *88*, 563.